Hindawi
Wireless Communications and Mobile Computing
Volume 2021, Article ID 5529655, 7 pages
https://doi.org/10.1155/2021/5529655

Research Article

Modulation of the Transmission Spectra of the Double-Ring Structure by Surface Plasmonic Polaritons

Senfeng Lai,[1] **Yanpei Guo**,[1] **Guiyang Liu**,[1] **Chun Shan**,[1] **Lixin Huang**,[1] **Yicong Zhang**,[1] **Yanghui Wu**,[2] **Wenhua Gu**,[2] **and Wen Wu**[2]

[1]*School of Electronic and Information, Guangdong Polytechnical Normal University, Guangzhou 510635, China*
[2]*School of Electronic and Optical Engineering, Nanjing University of Science and Technology, Nanjing 210094, China*

Correspondence should be addressed to Chun Shan; shanchun@gpnu.edu.cn

Received 5 February 2021; Revised 22 February 2021; Accepted 3 April 2021; Published 15 April 2021

Academic Editor: zhihong tian

This paper proposes a new structural design to excite surface plasmonic polaritons to enhance the double-ring interference structure. The double-ring structure was etched into a thin film to form fundamental interference patterns, and periodic concentric-ring grooves were employed to gather energy from the surrounding regions through the excitation of surface plasmonic polaritons. Accordingly, the energy of the incident light can be concentrated at the center. The surface plasmon modulates the interference pattern and the transmission spectra. The transmission peak position and its intensity can be tuned by changing the alignment of the grooves. The proposed structure can be applied for designing plasmonic devices as useful components of the plasmonic toolbox.

1. Introduction

With the development of Internet of things and cloud technology, the amount of data that modern communication needs to process is becoming more and more huge [1–5]. In order to improve the communication bandwidth, more and more communication networks choose optical fiber transmission. In the optical transmission, how to increase the light intensity has become a hot topic. The double-slit interference experiment has been known as one of the most profound experiments in physics since the last century. However, surface plasmonic polaritons (SPPs), as a hot research topic owing to their energy enhancement effect at a specific wavelength, are a relatively new concept in physics. The combination of surface plasmonic polaritons and double-slit interference is an exciting research topic [6–20]. The outcomes have potential applications in quantum physics, fundamental optics, optical imaging, detection, integrated circuit design, and other fields [21–28].

In this paper, a new double-ring structure, as shown in Figures 1(a) and 1(b), is proposed to combine the double-slit interference with SPPs to explore exciting possibilities. The proposed structure is a double-ring structure formed by the combination of the periodic concentric-ring grooves [7, 15] and a modified version of Young's double-slit structure and allows for a strong interaction between the two substructures. In the structures shown in Figures 1(a) and 1(b), two concentric rings are shown etched into a silver thin film to make scope for a fundamental double-ring interference. A series of periodic concentric-ring grooves was etched into both the upper and lower surfaces of a silver film to stimulate surface plasmonic polaritons.

Simulations were used to study the transmitted interference pattern and the transmission spectrum of the proposed structure based on the finite difference time domain (FDTD) method. The standout feature of the proposed structure is that it makes use of the classic bull's eye structure to efficiently gather the energy from the surrounding areas and supply it to the center of the interference pattern. It also contains many geometric factors for adjusting and fine-tuning the transmission results. Both the interference pattern and the transmission spectrum were studied.

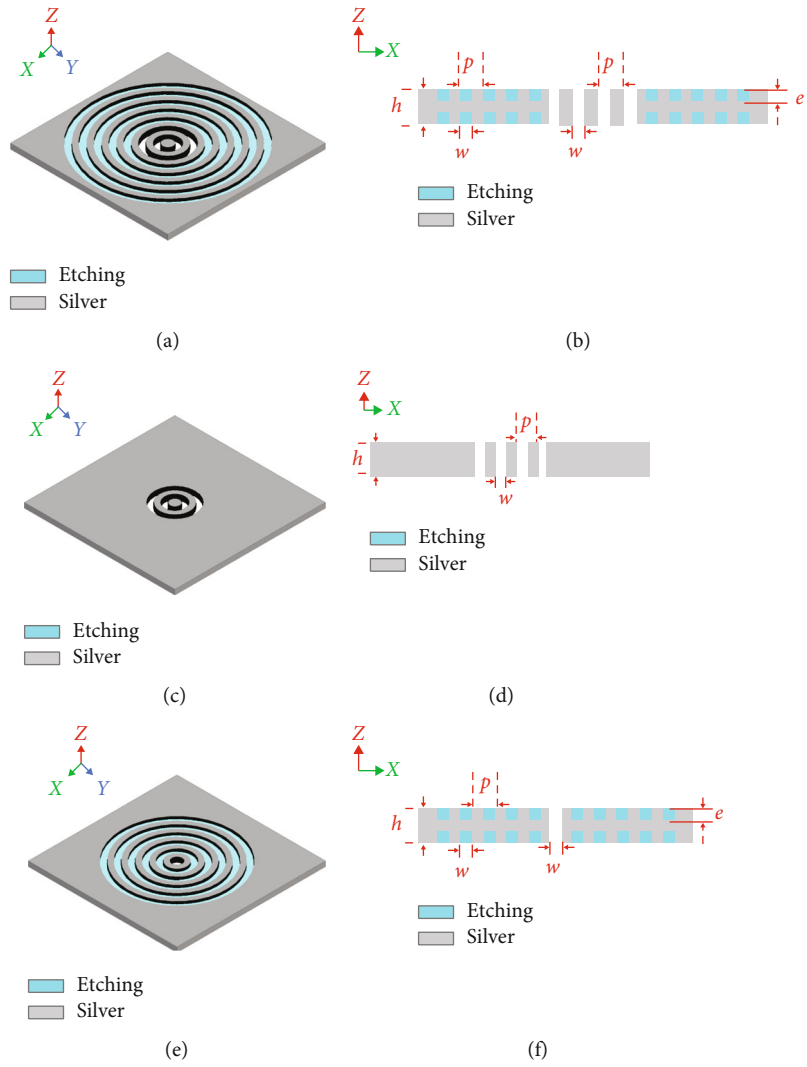

Figure 1: Schematic diagram of the proposed structure: double-ring aperture at the center of the silver film surrounded by periodic concentric-ring grooves, top view (a) and side view (b); schematic diagram of the reference aperture-only structure: double-ring aperture at the center of the silver film, top view (c) and side view (d); schematic diagram of the bull's eye structure, top view (e) and side view (f).

2. Precise Modulation of the Transmission Spectrum of the Concentric-Ring Interference

The proposed structure is displayed in Figures 1(a) (top view) and 1(b) (side view). The silver thin film consists of two concentric-ring apertures at the center, and a series of periodic concentric-ring grooves was etched into the thin film from both sides. The concentric-ring pitch was $p = 600$ nm and the width was $w = 300$ nm, for the center apertures as well as the surrounding grooves. The groove depth was $e = 60$ nm on each side, and the thickness of the thin film before etching was $h = 300$ nm. The reference aperture-only structure was also studied as a comparison, as shown in Figures 1(c) (top view) and 1(d) (side view). The standard bull's eye structure, which contained only one round aperture at the center as shown in Figures 1(e) (top view) and 1(f) (side view), had the same concentric-ring grooves in the surroundings as in Figures 1(a) and 1(c). The radius of the central aperture was 300 nm. The surrounding medium was air. All the other conditions were kept identical for the above three structures. The incident light was a plane wave transmitted under the thin film from the $-z$-direction to the $+z$-direction. The finite difference time-domain (FDTD) method

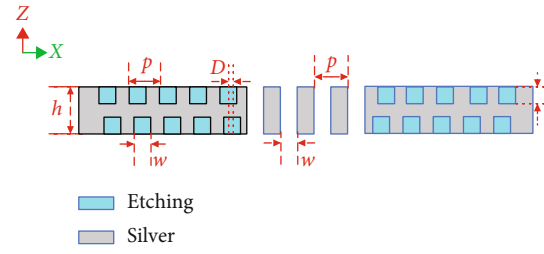

Figure 2: Modification of the relative position of the upper and lower concentric rings.

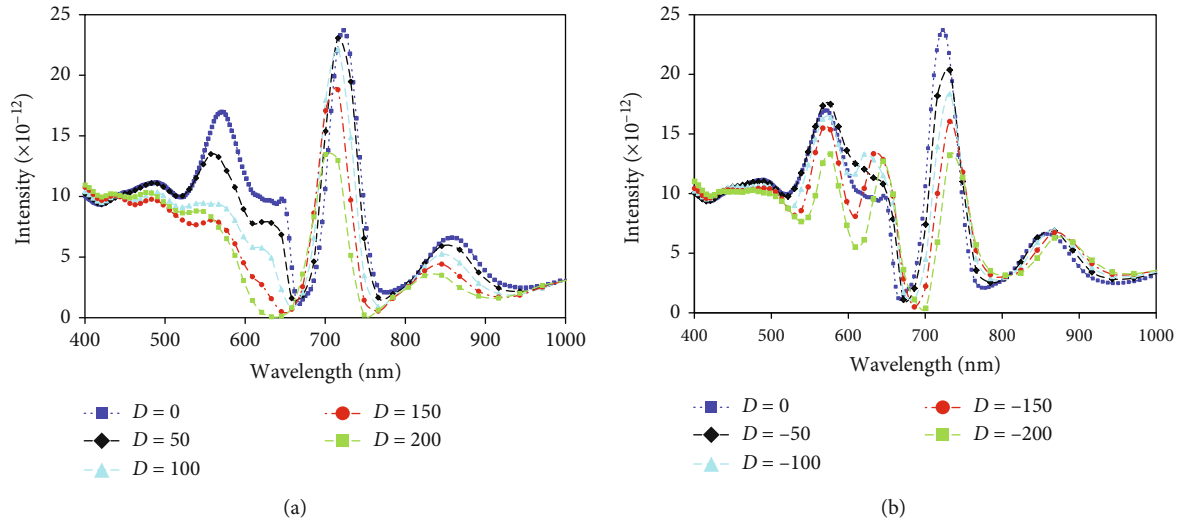

Figure 3: Transmission spectra in the far-field region at 0° collection angle for different values of D: (a) $D > 0$ and (b) $D < 0$.

was used to calculate the EM field intensity and distribution before and after the incident light hit the studied structures.

Based on the structure shown in Figures 1(a) and 1(b), some more geometric modifications were applied to the structure. The most exciting modification was found to be the impact of the relative position of the upper and lower concentric-ring grooves. As shown in Figure 2, the relative distance between the centers of the upper and lower adjacent concentric rings was defined as D, and 0 for the symmetric structures shown in Figure 1. For a positive value of D, the lower concentric-ring grooves remained closer to the center than the upper ones; while for a negative value of D, the opposite observation was recorded.

The transmission spectra shown in Figure 3 were obtained by varying the values of D within the range of -200 nm to +200 nm, while other parameters (film thickness, etching depth, concentric ring period, and the number of the concentric rings, etc.) remained unchanged. Since our structure is perfectly symmetrical, the optical wave simulation in this paper will not produce the phenomenon of polarization conversion.

Figure 3 reveals that when the relative distance D is greater than 0, the peak wavelength of the transmission spectrum experiences a blueshift. With the increase in the relative distance D, the magnitude of the blueshift increases, in addition to the decrease in peak field intensity. When D is less than 0, the peak wavelength of the transmission spectrum is redshifted. With the decrease in the relative position of D, the redshift magnitude increases, while the peak field intensity decreases. For further analysis of the relationship between the peak wavelength shift and D, the former is plotted as the y-axis against the latter as the x-axis in Figure 4. The relationship between the peak field intensity and D is plotted in Figure 5.

From Figure 4, it is obvious that the peak wavelength shift and the relative distance D have a near-linear relationship, and the fitting formula is in

$$\text{shift wavelength} = -0.0839 \times D - 0.2182. \quad (1)$$

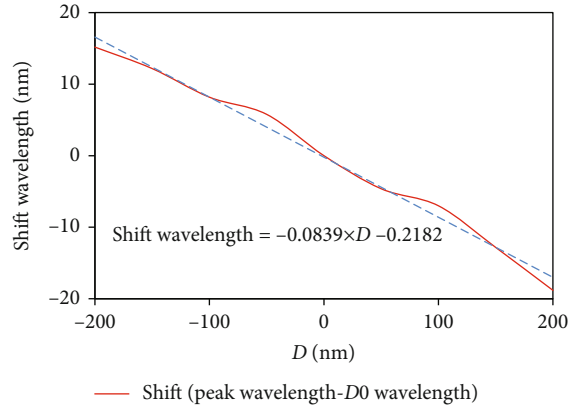

Figure 4: Relationship between the peak wavelength shift and D.

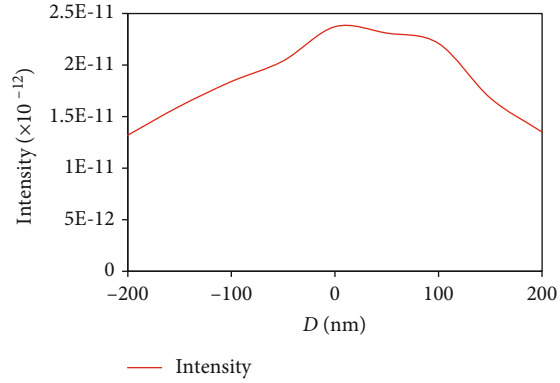

Figure 5: Relationship between the peak intensity and D.

The relationship curve is symmetric to the original point, which can be very useful and convenient in potential applications. It is well-known that both the upper and lower concentric-ring grooves can generate surface plasmonic waves. The final transmission peak arises as a result of the superposition and resonance of these waves. When the value of$D$is greater than 0, i.e., the lower grooves come closer to the

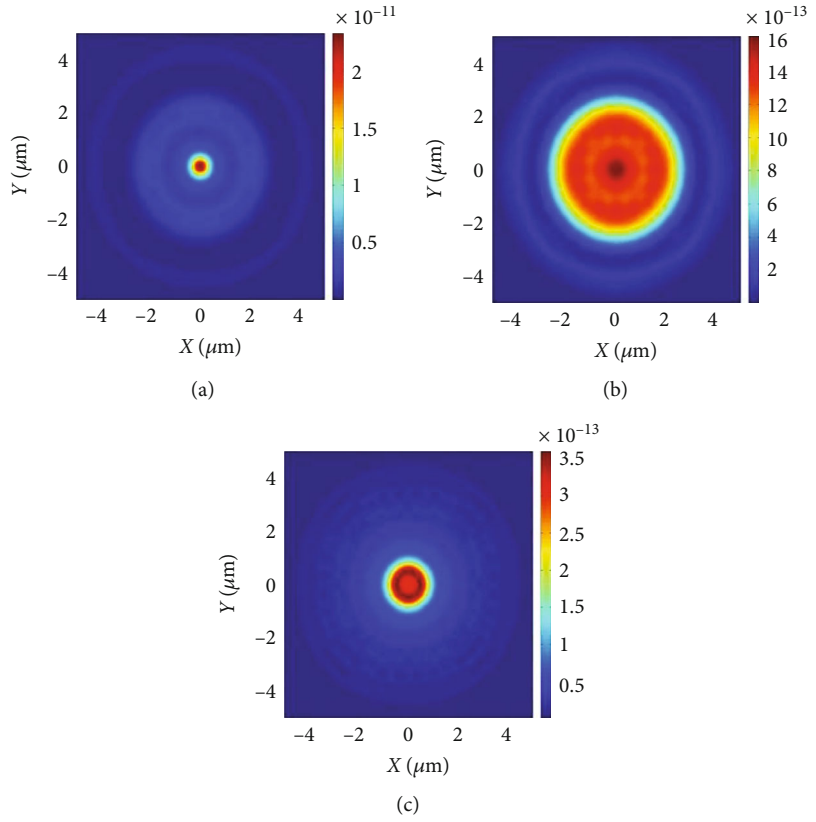

Figure 6: Far field of the film at 715 nm for (a) the proposed structure, (b) the reference aperture-only structure, and (c) the bull's eye structure.

center, this leads to the reduction in the effective aperture width of the lower structure. The aperture gets narrower for the entire structure, leading to a shorter peak wavelength, thus being blueshifted. Likewise, when the value of$D$is less than 0, i.e., the lower grooves tend to go further away from the center, and the effective aperture width of the lower structure gets wider for the entire structure, this leads to a longer peak wavelength, and hence is redshifted.

Figure 5 is easy to understand. The plasmonic wave produced by upper and lower concentric-ring grooves displays identical properties since the geometries and materials are all the same. When the upper and lower grooves get aligned ($D = 0$), the two surface plasmonic waves resonate. Thus, the highest transmission is generated. As a result, the peak transmission reaches a maximum when $D = 0$. The shift from the aligned position ($D > 0$ or $D < 0$) destroys the resonance and causes a decrease in the transmission intensity.

3. Details of the Interference Pattern Subheadings

Since the transmission spectrum was modulated by a double-ring structure, a valid question arose about the process of change of the interference patterns for the proposed structure. The detailed interference patterns of the three structures shown in Figure 1 produced results based on which this question could be answered. The detailed discussion is presented in the following subsections.

3.1. Enhancement of the Interference Patterns. The far-field intensity patterns at 715 nm are shown in Figure 6. Figure 6(a) is the far-field pattern of the proposed structure, Figure 6(b) is the reference aperture-only structure, and Figure 6(c) is that of the bull's eye structure [4]. After adding a series of concentric rings in the surroundings, the intensity of the transmitted spectrum gets noticeably concentrated in the central area of the proposed structure, and the intensity at the center increases by one order of magnitude. Moreover, tightly squeezed circular interference fringes are produced by the proposed structure, as compared to the aperture-only structure. The proposed structure has the largest electric field intensity.

The corresponding angle dependence relationship at 715 nm can be a more precise description of the pattern squeeze, as shown in Figure 7.

Figure 7(a) displays the near 20-fold increase in the transmitted light intensity magnitude of the proposed structure versus the aperture-only structure. Figure 7(b) displays the normalized angle dependence, which clearly demonstrates that the distribution of the side lobes in the transmission pattern is practically the same for the two structures, and the crucial difference lies in the distribution of light intensity. The light intensity is highly concentrated in the main lobe for the proposed structure, which is nearly 10 times higher than the first side lobe pair. In contrast, the first side lobe pair is nearly 85% of the main lobe in the aperture-only structure.

This squeezed pattern is attributable to the strong resonance of the stimulated SPPs with the double-ring

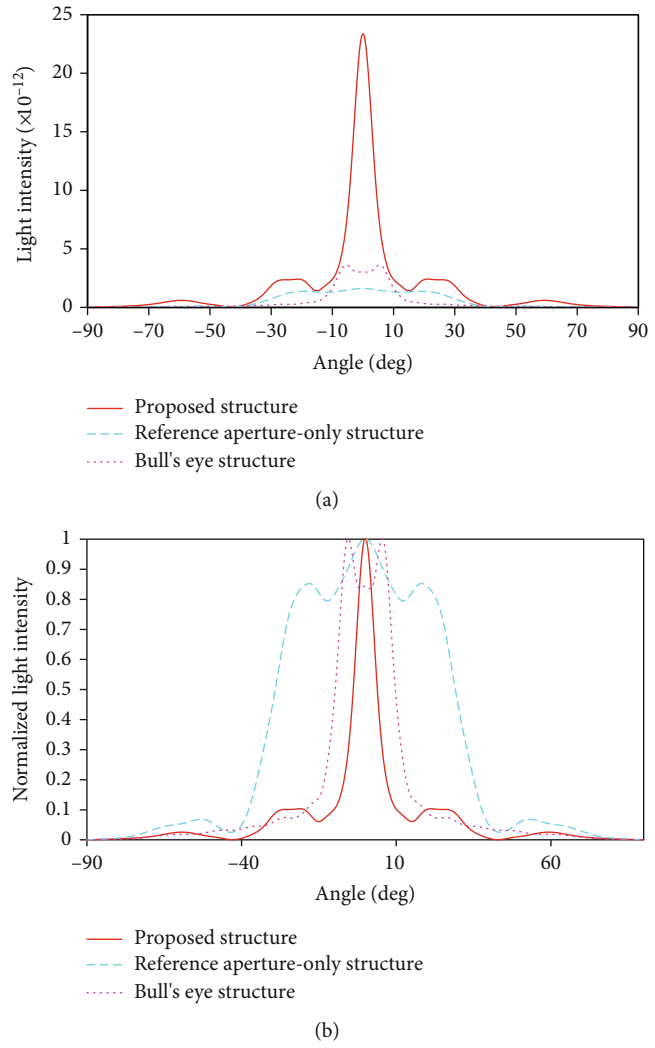

FIGURE 7: The angle dependence of the transmission light intensity at 715 nm of the structure: original data (a) and normalized data (b).

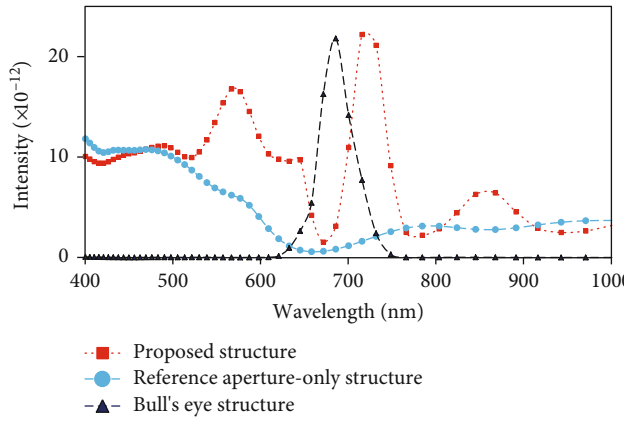

FIGURE 8: Transmission spectra for the three structures studied in the far-field region at 0° collection angle. Color code: red squares joined by red line: proposed structure; blue dots joined by blue line: aperture-only structure; purple triangles joined by purple line: bull's eye structure.

interference and can be useful in certain applications, including high-energy physics and coherent laser light focusing.

3.2. Enhancement of the Transmission Spectra. The transmission spectra of the three structures studied at a collection angle of 0° are shown in Figure 8.

From Figure 8, it can be clearly understood that in the aperture-only structure, the transmission spectrum curve is comparatively flat, with a few shallow ups and downs, but without any evident frequency-selectivity characteristics. While the bull's eye structure displays one clear transmission peak at 685 nm, transmission at other wavelengths is negligible. The proposed structure displays combined characteristics of the aperture-only structure and bull's eye structure, with signs of enhanced power transmission as well as stronger interference. Understanding of the transmission spectrum of the proposed structure is based on the following concepts: the double-ring aperture controls the interference patterns over the whole wavelength range, but the SPP effect takes place only at a specific SPP frequency, as evident from the transmission peak of the bull's eye structure. Therefore, supervision of the two structures, i.e., the proposed structure in this work, shows the fundamental interference patterns as the background, with strong modification by SPP around the SPP wavelength.

A more careful observation of the transmission spectra indicates that the total transmission power of the proposed structure is greater than the aperture-only structure, implying a much higher energy-collection capability. The peak intensity for the proposed structure is roughly twice of the aperture-only structure. This is because the SPP mode gets excited by the surrounding grooves that result in efficient collection of the surrounding energy.

The redshift of the transmission peak of the proposed structure from 685 nm to 715 nm, as compared to the bull's eye structure, is an interesting observation. This phenomenon most likely occurs because the concentric-ring in the center can become equivalent to the wider aperture in the bull's eye structure. As it is well-known, for bull's eye structures, the wider the central through-aperture is, the longer the peak wavelength will be.

4. Conclusions

In this paper, a new structure was proposed by combining the double-ring structure for interference with the bull's eye structure for SPP stimulation. It was observed that the new structure could introduce a stronger interference pattern and modify the transmission spectrum, which led to some interesting results. By altering the relative position of the upper and lower periodic grooves, both the intensity and the position of the peak of the transmission spectrum could be precisely adjusted. The results are useful in potential applications in both fundamental physics and applied optics.

Data Availability

The detailed parameter data of this article has been listed in the paper; according to this data, everyone can get the results of this paper.

Conflicts of Interest

The authors declare that there is no conflict of interest regarding the publication of this paper.

Acknowledgments

This work is supported by the Young Innovative Talents Project, Guangdong Province (No. 2019KQNCX069); Special Fund for Science and Technology Innovation Strategy of Guangdong Province (Climbing plan, pdjh2020b0344); Guangzhou Science and Technology Innovation Development Special Fund Project; and National Key R&D Program of China–Industrial Internet Application Demonstration-Sub-Topic Intelligent Network Operation and Security Protection (2018YFB1802402).

References

[1] J. Qiu, Z. Tian, C. Du, Q. Zuo, S. Su, and B. Fang, "A survey on access control in the age of internet of things," *IEEE Internet of Things Journal*, vol. 7, no. 6, pp. 4682–4696, 2020.

[2] J. M. Yi, A. Cuche, E. Devaux, C. Genet, and T. W. Ebbesen, "Beaming visible light with a plasmonic aperture antenna," *ACS Photonics*, vol. 1, no. 4, pp. 365–370, 2014.

[3] P. Chen, C. Chen, S. Qin et al., "Efficient planar plasmonic directional launching of linearly polarized light in a catenary metasurface," *Physical Chemistry Chemical Physics*, vol. 22, no. 47, pp. 27554–27559, 2020.

[4] C. Cen, H. Lin, C. Liang et al., "Tunable plasmonic resonance absorption characteries-tics in periodic H-shaped graphene arrays," *Superlattices and Microstructures*, vol. 120, pp. 427–435, 2018.

[5] B. Eftekharinia, "Highly confined long range transmission of a surface plasmon polariton mode in a novel design of metallic slit-groove nanostructures," *Optik*, vol. 194, p. 163103, 2019.

[6] S. Basudeb, K. Roy, B. Yaara, and P. Yehiam, "Plasmonic flat surface Fabry-Perot interferometry," *Nanophotonics*, vol. 7, no. 3, pp. 635–641, 2018.

[7] B. Hauer, C. E. Marvinney, M. Lewin et al., "Exploiting phonon-resonant near-field interaction for the nanoscale investigation of extended defects," *Advanced Functional Materials*, vol. 30, no. 10, p. 1907357, 2020.

[8] B. Zhao and J. Yang, "New effects in an ultracompact Young's double nanoslit with plasmon hybridization," *New Journal of Physics*, vol. 15, no. 7, article 073024, 2013.

[9] G. Matan, S. Omer, W. Adam, A. Hannah, and G. David, "Second harmonic generation hotspot on a centrosymmetric smooth silver surface," *Light Science & Applications*, vol. 7, no. 1, article 49, 2018.

[10] H. Li, Y. Xu, G. Wang, T. Fu, L. Wang, and Z. Zhang, "Converting surface plasmon polaritons into spatial bending beams through graded dielectric rectangles over metal film," *Optics Communications*, vol. 383, pp. 423–429, 2017.

[11] G. Li and Q. Xiong, "Scattering by abrupt discontinuities on photonic nanowires: closed-form expressions for domain reduction," *Optics Express*, vol. 22, no. 21, pp. 25137–25148, 2014.

[12] G. Soavi, G. Wang, H. Rostami et al., "Broadband, electrically tunable third-harmonic generation in graphene," *Nature Nanotechnology*, vol. 13, no. 7, pp. 583–588, 2018.

[13] Z. Tian, C. Luo, J. Qiu, X. Du, and M. Guizani, "A distributed deep learning system for web attack detection on edge devices," *IEEE Transactions on Industrial Informatics*, vol. 16, no. 3, pp. 1963–1971, 2020.

[14] C. S. Perera, K. C. Vernon, A. M. Funston, H. Cheng, F. Eftekhari, and T. J. Davis, "Excitation of bound plasmons along nanoscale stripe waveguides: a comparison of end and grating coupling techniques," *Optics Express*, vol. 23, no. 8, pp. 10188–10197, 2015.

[15] H. Zhu, T. Xu, Z. Wang et al., "Flat metasurfaces to collimate electromagnetic waves with high efficiency," *Optics Express*, vol. 26, no. 22, pp. 28531–28543, 2018.

[16] M. Li, Y. Sun, H. Lu, S. Maharjan, and Z. Tian, "Deep reinforcement learning for partially observable data poisoning attack in crowdsensing systems," *IEEE Internet of Things Journal*, vol. 7, no. 7, pp. 6266–6278, 2020.

[17] J. Long, H. Yi, H. Li, Z. Lei, and T. Yang, "Reproducible ultrahigh SERS enhancement in single deterministic hotspots using nanosphere-plane antennas under radially polarized excitation," *Scientific Reports*, vol. 6, no. 1, article 33218, 2016.

[18] F. A. Koenderink, "Single-photon nanoantennas," *ACS Photonics*, vol. 4, no. 4, pp. 710–722, 2017.

[19] J. Bland-Hawthorn, M. Sellars, and J. Bartholomew, "Quantum memories and the double-slit experiment: implications for astronomical interferometry," 2021, https://arxiv.org/abs/2103.07590.

[20] J. Qi, T. Kaiser, A. E. Klein et al., "Enhancing resonances of optical nanoantennas by circular gratings," *Optics Express*, vol. 23, no. 11, pp. 14583–14595, 2015.

[21] L. Zheng, U. Zywietz, A. Evlyukhin, B. Roth, L. Overmeyer, and C. Reinhardt, "Experimental demonstration of surface plasmon polaritons reflection and transmission effects," *Sensors*, vol. 19, no. 21, p. 4633, 2019.

[22] Z. Li, Y. Sun, K. Wang et al., "Tuning the dispersion of effective surface plasmon polaritons with multilayer systems," *Optics Express*, vol. 26, no. 4, pp. 4686–4697, 2018.

[23] Y. P. Qi, P. Y. Zhou, X. W. Zhang, C. M. Yan, and X. X. Wang, "Enhanced optical transmission by exciting hybrid states of Tamm and surface plasmon polaritons in single slit with multi-pair groove nanostructure," *Acta Physica Sinica*, vol. 67, no. 10, article 107104, 2018.

[24] S. Wang, X. Wang, and Y. Zhang, "Simultaneous airy beam generation for both surface plasmon polaritons and transmitted wave based on metasurface," *Optics Express*, vol. 25, no. 20, pp. 23589–23596, 2017.

[25] M. Shafiq, Z. Tian, A. K. Bashir, X. Du, and M. Guizani, "CorrAUC: a malicious Bot-IoT traffic detection method in IoT network using machine-learning techniques," *IEEE Internet of Things Journal*, vol. 8, no. 5, pp. 3242–3254, 2021.

[26] T. Zhang, C. Wang, H. Chen et al., "Controlled multichannel surface plasmon polaritons transmission on atomic smooth silver triangular waveguide," *Advanced Optical Materials*, vol. 7, no. 21, p. 1900930, 2019.

[27] Z. Tian, X. Gao, S. Su, and J. Qiu, "Vcash: a novel reputation framework for identifying denial of traffic service in internet of connected vehicles," *IEEE Internet of Things Journal*, vol. 7, no. 5, pp. 3901–3909, 2020.

[28] H. Sun, Y. Zhu, B. Gao, P. Wang, and Y. Yu, "Polarization-dependent quasi-far-field superfocusing strategy of nanoring-based plasmonic lenses," *Nanoscale Research Letters*, vol. 12, no. 1, p. 386, 2017.